

## Compensating for Variations in $^1\text{H}$ – $^{13}\text{C}$ Scalar Coupling Constants in Isotope-Filtered NMR Experiments

Ashley C. Stuart,<sup>†</sup> Kris A. Borzilleri,<sup>‡</sup> Jane M. Withka,<sup>‡</sup> and Arthur G. Palmer III<sup>\*†</sup>

Department of Biochemistry and Molecular Biophysics  
Columbia University, New York, New York 10032  
Exploratory Medicinal Sciences  
Pfizer Central Research  
Groton, Connecticut 06430

Received December 3, 1998

Revised Manuscript Received April 23, 1999

Isotope-filtered experiments are essential to the study of biomolecular complexes by NMR spectroscopy because they permit selective observation of unlabeled molecules in the presence of isotopically enriched proteins or nucleic acids.<sup>1</sup> Isotope filters rely on evolution of  $^1\text{H}$  coherences under the heteronuclear scalar coupling Hamiltonian to suppress signals arising from  $^1\text{H}$  spins in  $^{13}\text{C}$ – $^1\text{H}$  moieties; consequently, the variation in one-bond  $J_{\text{CH}}$  scalar coupling constants in proteins compromises performance. In this paper, we present a new filtering strategy based on the isomorphism between broadband polarization transfer and composite pulse rotations.<sup>2,3</sup> The new approach does not rely on double-tuned filter elements<sup>4,5</sup> or on empirical correlations between the  $^{13}\text{C}$  chemical shift and  $J_{\text{CH}}$ .<sup>6,7</sup> In addition, the entire filter period can be used for frequency labeling in a semiconstant time manner<sup>8</sup> to provide increased resolution in the indirect  $^1\text{H}$  evolution dimension of multidimensional F1-filtered NMR spectra. The new approach is demonstrated in an F1-filtered, F2-edited  $^1\text{H}$ – $^{13}\text{C}$  NOESY-HSQC experiment applied to the complex between unlabeled FK506 and [U-98%  $^{13}\text{C}$ , U-98%  $^{15}\text{N}$ ]-labeled FKBP-12.

Rotations in the operator space  $\{I_x, I_y, I_z\}$  generated by on-resonance radio frequency pulses are isomorphous to rotations in the operator space  $\{2I_xS_z, I_y, 2I_zS_z\}$  generated by the scalar coupling Hamiltonian, in which  $I = ^1\text{H}$  and  $S = ^{13}\text{C}$ .<sup>2,3</sup> Thus, a composite  $90^\circ$  pulse that compensates for variations in the nominal rotation angle can be converted into a pulse-interrupted-free-precession period that transforms  $I_y$  magnetization into two-spin operators independently of the variation in  $J_{\text{CH}}$ . The pulse sequence of Figure 1a is derived from the  $90^\circ$  composite pulse  $(\beta)_0(2\beta)_{2\pi/3}$ ,<sup>9</sup> in which the bracketed term is the nominal rotation angle, the subscript is the phase of the pulse, and  $\beta \approx \pi/2$ . If the initial state of the density operator is proportional to  $I_y$ , the final density operator is proportional to  $\epsilon I_y$ , in which the efficiency of the filter is given by

$$\epsilon = \cos(\pi J_{\text{CH}}\tau) \cos(2\pi J_{\text{CH}}\tau) + 0.5 \sin(\pi J_{\text{CH}}\tau) \sin(2\pi J_{\text{CH}}\tau) = \cos^3(\pi J_{\text{CH}}\tau) \quad (1)$$

\* Corresponding author. Voice: (212) 305-8675. Fax: (212) 305-7932. E-mail: agp6@columbia.edu.

<sup>†</sup> Columbia University.

<sup>‡</sup> Pfizer Central Research.

(1) Otting, G.; Wüthrich, K. *Q. Rev. Biophys.* **1990**, *23*, 39–96.  
(2) Garbow, J. R.; Weitekamp, D. P.; Pines, A. *Chem. Phys. Lett.* **1982**, *504*, 504–509.

(3) Levitt, M. H. *Prog. Nucl. Magn. Reson. Spectrosc.* **1986**, *18*, 61–122.  
(4) Gemmecker, G.; Oleiniczak, E. T.; Fesik, S. W. *J. Magn. Reson.* **1992**, *96*, 199–204.

(5) Ikura, M.; Bax, A. *J. Am. Chem. Soc.* **1992**, *114*, 2433–2440.

(6) Kupce, E.; Freeman, R. *J. Magn. Reson.* **1997**, *127*, 36–48.

(7) Zwaalen, C.; Legault, P.; Vincent, S. J. F.; Greenblatt, J.; Konrat, R.; Kay, L. E. *J. Am. Chem. Soc.* **1997**, *119*, 6711–6721.

(8) Grzesiek, S.; Bax, A. *J. Biomol. NMR* **1993**, *3*, 185–204.

(9) Levitt, M. H. *J. Magn. Reson.* **1982**, *48*, 234–264.

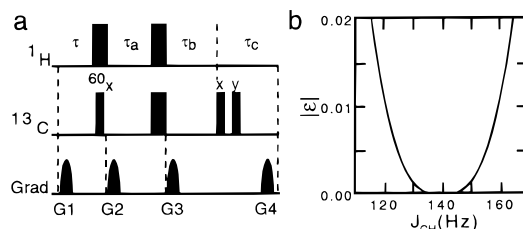


**Figure 1.**  $J$ -compensated isotope filter. (a) The basic filter sequence element is illustrated. Unless otherwise noted, narrow and wide filled rectangles denote  $90^\circ$  and  $180^\circ$  pulses, respectively. The delays are  $\tau = 1/(2J_0)$  and  $\tau_a = 1.5\tau + 0.5\tau_c$ ,  $\tau_b = 0.5(\tau - \tau_c)$ , and  $\tau_c$  is long enough to encompass the final two  $^{13}\text{C}$  pulses and gradient pulse G4.  $J_0$  is the nominal coupling constant for which the filter is tuned. The four gradients satisfy  $\tau_1A_1 - \tau_2A_2 + \tau_3A_3 + \tau_4A_4 = 0$ , in which  $\tau_k$  and  $A_k$  are the duration and amplitude of the  $k$ th gradient pulse  $G_k$ , respectively. (b) Isotope filter efficiency. The solid line shows a plot of the absolute value of the filter efficiency given by eq 1 for a nominal  $J_0 = 140$  Hz.

and the filter is tuned for a nominal scalar coupling constant  $J_0 = 1/(2\tau)$ . The simultaneous  $180^\circ$   $^1\text{H}$  and  $60^\circ$   $^{13}\text{C}$  pulses in Figure 1a could be replaced by a single  $120^\circ$   $^{13}\text{C}$  pulse; however, the off-resonance effects of a  $60^\circ$   $^{13}\text{C}$  pulse are negligible.<sup>10</sup> If the I spins are not scalar-coupled to a  $^{13}\text{C}$  spin, then  $J_{\text{CH}} = 0$  and  $\epsilon = 1$ . If the I spins are scalar-coupled to a  $^{13}\text{C}$  spin with  $J_{\text{CH}} \approx J_0$ , then  $\epsilon \approx (\pi/2)^3(1 - J_{\text{CH}}/J_0)^3$  and  $|\epsilon| \leq 0.02$  is obtained for a variation  $|1 - J_{\text{CH}}/J_0| \leq 0.17$ . The dependence of the filter efficiency calculated using eq 1 is shown in Figure 1b for a nominal  $J_0 = 140$  Hz. High suppression efficiency is observed for  $J_{\text{CH}}$  over the range 115–165 Hz; therefore, this isotope filter is sufficiently broadband to obtain efficient purging of all  $^{13}\text{C}$ -attached  $^1\text{H}$  spins in proteins, except those in His imidazole groups.

Figure 2 illustrates the incorporation of the new isotope filter into an F1-filtered, F2-edited  $^1\text{H}$ – $^{13}\text{C}$  NOESY-HSQC experiment. Because the filter element does not contain any  $^1\text{H}$   $90^\circ$  pulses, magnetization from  $^{12}\text{C}$ -attached  $^1\text{H}$  spins is frequency-labeled using the semiconstant time technique<sup>8</sup> by varying  $\tau_a$ ,  $\tau_b$ , and  $\tau_c$  as described in the figure caption. The apparent decay rates and homonuclear coupling constants for  $^1\text{H}$  magnetization thereby are reduced by a factor of  $1 - 3\tau/t_{1\text{max}}$ , in which  $t_{1\text{max}}$  is the maximum value of the indirect evolution period. This effect both increases the resolution of the spectrum and partially compensates for the increased length of the new filter element ( $\sim 3\tau$ ) compared with that of a conventional double-tuned filter ( $\sim 2\tau$ ).<sup>4,5</sup> After the isotope filter and evolution period, magnetization is returned to the  $z$  axis for the NOESY mixing period. A standard  $^1\text{H}$ – $^{13}\text{C}$  HSQC sequence is used for F2  $^{13}\text{C}$  editing and F3 detection.

To validate the proposed method, an F1-filtered, F2-edited  $^1\text{H}$ – $^{13}\text{C}$  NOESY-HSQC spectrum was recorded for the complex between the unlabeled macrolide FK506 and [U-98%  $^{13}\text{C}$ , U-98%  $^{15}\text{N}$ ]-labeled FKBP-12.<sup>11</sup> Figure 3a and b show NOEs from FK506 to a Tyr ring system, which has been assigned as Tyr 82 on the basis of previous reports.<sup>12,13</sup> Diagonal peaks are folded in this spectrum and would occur at  $-1.1$  and  $-1.8$  ppm in Figures 3a and 3b, respectively; no signals are observed at these shifts due to the efficiency of the filter. Figure 3c shows NOEs from His 87, the only His in the binding pocket, to FK506. Diagonal peaks are seen at  $-0.58$  ppm because  $J_{\text{CH}} = 200$  Hz for His is beyond

(10) Cavanagh, J.; Fairbrother, W. J.; Palmer, A. G.; Skelton, N. J. *Protein NMR Spectroscopy: principles and practice*; Academic Press: San Diego, CA, 1996; p 587.

(11) Schreiber, S. *Science (Washington, D.C.)* **1991**, *251*, 283–287.

(12) VanDuyne, G. D.; Standaert, R. F.; Karplus, P. A.; Schreiber, S. L.; Clardy, J. *Science (Washington, D.C.)* **1991**, *252*, 839–842.

(13) Lepre, C. A.; Thomson, J. A.; Moore, J. M. *FEBS Lett.* **1992**, *302*, 89–96.

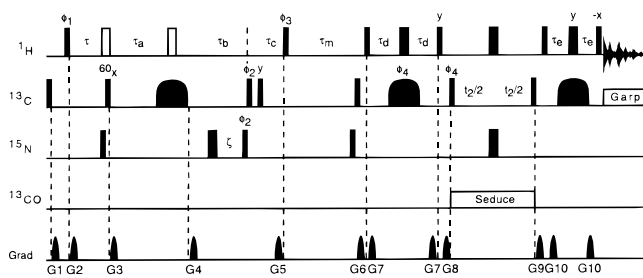


**Figure 2.** F1  $^{13}\text{C}$ -filtered, F2  $^{13}\text{C}$ -edited NOESY-HSQC J-compensated pulse sequence. Narrow and wide rectangles correspond to  $90^\circ$  and  $180^\circ$  pulses unless otherwise noted. Unfilled  $180^\circ$   $^1\text{H}$  pulses represent  $90_x$ - $180_y$ - $90_x$  composite  $180^\circ$  pulses. The wide, rounded rectangles represent adiabatic or composite  $180^\circ$   $^{13}\text{C}$  pulses for inversion over the full spectral width from aromatic to methyl resonances. The  $^{13}\text{C}$  hard pulses are applied at an offset of 72.5 ppm with  $\gamma B_1 = 16.7$  kHz. The  $^1\text{H}$  pulses are applied with  $\gamma B_1 = 24$  kHz centered on the  $\text{H}_2\text{O}$  resonance. Nitrogen pulses are applied at an offset of 118 ppm with  $\gamma B_1 = 6.67$  kHz. Carbonyl decoupling during the  $t_2$  period employs a cosine-modulated seduce pulse shape with  $\gamma B_1 = 3.4$  kHz and the WALTZ-16 supercycle.<sup>15</sup> Carbon decoupling during acquisition is achieved with GARP phase modulation and  $\gamma B_1 = 5$  kHz.<sup>16</sup> For a nominal scalar coupling,  $J_0 = 140$  Hz, the delays are  $\tau = 3.57$  ms,  $\tau_a = 5.355$  ms +  $0.5 \tau_{c0} - n\Delta\tau$ ,  $\tau_b = 0.5(3.57$  ms -  $\tau_{c0}) + n\Delta\tau$ ,  $\tau_c = \tau_{c0} + n(1/\text{SW1} - 2\Delta\tau)$ ,  $\Delta\tau = (5.425$  ms -  $\tau_{a0})/(N-1)$ ,  $\tau_{a0} = 0.9$  ms is the minimum value of  $\tau_a$  (as a result of G3 and the  $^{13}\text{C}$  inversion pulse),  $\tau_{c0} = 0.65$  ms is the minimum value of  $\tau_c$  (as a result of the  $^{13}\text{C}$   $90^\circ$  pulses and G5),  $\tau_d = 1.785$  ms, and  $\tau_e = 1.785$  ms, in which N is the total number of  $t_1$  increments,  $0 \leq n < N$ , and SW1 is the spectral width in the F1 dimension. The filter efficiency for  $^1\text{H}^{\text{N}}$  spins is  $\cos(\pi J_{\text{NH}}\tau)\cos[\pi J_{\text{NH}}(\tau_a - \tau_b + 2\zeta)]$  and is optimized by setting  $\tau_a - \tau_b + 2\zeta = 1/(2J_{\text{NH}})$ , in which  $J_{\text{NH}}$  is the one-bond  $^1\text{H}^{\text{N}}-^{15}\text{N}$  scalar coupling constant. The NOESY mixing time is  $\tau_m$ . In the present case,  $^{13}\text{C}$  inversion was obtained using a WURST adiabatic pulse<sup>17</sup> with a peak  $\gamma B_1 = 8.4$  kHz, a 60 kHz frequency sweep width, and a duration of 500  $\mu\text{s}$ . When using adiabatic inversion pulses, the filter efficiency for upfield (methyl) resonances can be improved slightly by empirically increasing  $\tau_a$  and  $\tau_b$  (by  $\sim 60$   $\mu\text{s}$ ) to account for the difference in inversion times at the edge and center of the  $^{13}\text{C}$  spectral range.<sup>6,7</sup> Gradient pulse lengths and strengths are G1 = (1.5 ms, 17 G/cm), G2 = (450  $\mu\text{s}$ , 10.4 G/cm), G3 = (450  $\mu\text{s}$ , 24 G/cm), G4 = (450  $\mu\text{s}$ , -13.8 G/cm), G5 = (450  $\mu\text{s}$ , 27.6 G/cm), G6 = (1 ms, 7 G/cm), G7 = (500  $\mu\text{s}$ , 7 G/cm), G8 = (500  $\mu\text{s}$ , 10.4 G/cm), G9 = (1.2 ms, -17.6 G/cm), G10 = (300  $\mu\text{s}$ , 20.7 G/cm). Gradients have the shape of the centerband of a sine function. The phase cycle is  $\phi_1 = (8 \times 45^\circ, 8 \times 225^\circ)$ ,  $\phi_2 = (x, -x)$ ,  $\phi_3 = (4x, 4(-x))$ ,  $\phi_4 = (2x, 2(-x))$ , receiver =  $(2x, 4(-x), 2x, 2(-x), 4x, 2(-x))$ .

the bandwidth of the filter. Diagonal peaks are recognizable as doublets with an apparent coupling  $J_{\text{CH}}(1 - 3\tau/t_{1\text{max}})$ . Empirically, the diagonal intensity from  $^{13}\text{C}$ -attached protons in the filtered spectrum is reduced by an average factor of 80 (40 for the methyl region of the spectrum) relative to that of an unfiltered NOESY-HSQC spectrum. Compared with a conventional double-filtered experiment (derived from Figure 3b of reference 7), the new experiment provides an average 4-fold improvement in filtration efficiency and reduces resonance line widths in F1 by 20%; however, the average signal-to-noise ratio for NOE cross-peaks is reduced on average by 10% as a result of the increased length of the pulse sequence.

A J-compensated isotope filter for purging signals from  $^1\text{H}$  spins that are scalar coupled to  $^{13}\text{C}$  spins has been developed through isomorphism to composite pulse rotations. The bandwidth

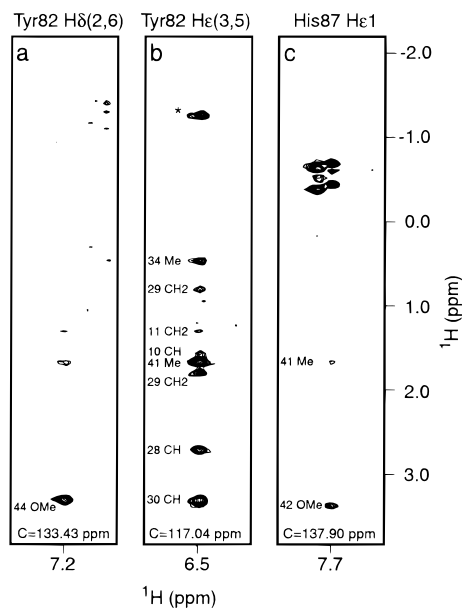


**Figure 3.** 3D F1  $^{13}\text{C}$ -filtered, F2  $^{13}\text{C}$ -edited NOESY-HSQC spectrum. F1/F3 slices at the indicated  $^{13}\text{C}$  F2 frequency are presented to illustrate NOEs from unlabeled FK506 (F1) to [ $^{13}\text{C}$ -98%,  $^{15}\text{N}$ -98%]-labeled FKBP-12 (F3). (a) NOEs to Tyr 82  $\text{H}\delta$  protons; the peak labeled \* is folded and has a chemical shift of 7.0 ppm. (c) NOEs to His 87  $\text{He}1$  proton. FK506 assignments have been published.<sup>13</sup> FK506 numbering is that used by the Cambridge Small Molecule Database. The sample was 1.44 of mM complex in 50 mM of potassium phosphate, 10%  $\text{D}_2\text{O}$ , 0.02% sodium azide, pH 6.8,  $T = 25^\circ\text{C}$ . The spectrum was recorded as a  $(128 \times 32 \times 512)$  point complex matrix with spectral widths of  $(5000 \times 4798 \times 10\,000)$  Hz using a Bruker DRX600 NMR spectrometer. The mixing time was 150 ms. The  $^{13}\text{C}$  carrier was set to 123 ppm during the mixing time to optimize the spectral width for aromatic  $^{13}\text{C}$  frequencies in F2. The spectrum was processed using Felix97 (Molecular Simulations, Inc.).

of the filter permits efficient suppression of all  $^{13}\text{C}$ -attached  $^1\text{H}$  spins in proteins other than His imidazole C-H moieties. In addition, enhanced resolution is obtained by incorporating a semiconstant time evolution period into the filter sequence. Finally, the filter efficiency does not depend on empirical correlations between  $^{13}\text{C}$  chemical shifts and  $J_{\text{CH}}$ ; therefore, this approach will be useful for performing isotope-filtered experiments in weakly aligned systems for which residual dipolar couplings contribute to the apparent coupling interaction.<sup>14</sup>

**Acknowledgment.** This work was supported in part by National Science Foundation (NSF) Grant MCB-9722392 (A.G.P.). A.C.S. was supported by a National Institutes of Health Grant 5T32 EY07105. Acquisition of the DRX600 spectrometer was supported by Grant NSF DBI-9601661.

JA984172W

(14) Tjandra, N.; Bax, A. *Science (Washington, D.C.)* **1997**, *278*, 1111–1114.

(15) McCoy, M.; Mueller, L. *J. Magn. Reson., Ser. A* **1993**, *101*, 122–130.

(16) Shaka, A. J.; Barker, P. B.; Freeman, R. *J. Magn. Reson.* **1985**, *64*, 547–552.

(17) Kupce, E.; Freeman, R. *J. Magn. Reson., Ser. A* **1995**, *115*, 273–276.